Tectonophysics 608 (2013) 499–504

Contents lists available at ScienceDirect

Tectonophysics

journal homepage: www.elsevier.com/locate/tecto

Strike-slip intraplate earthquakes in the Western Philippine Sea Plate

Jing-Yi Lin [a,*], Yen-Fu Chen [a], Chao-Shing Lee [b], Shu-Kun Hsu [a], Chin-Wei Liang [a,b], Yi-Chin Lin [a], Hsin-Sung Hsieh [a]

[a] Department of Earth Sciences and Institute of Geophysics, National Central University, 300 Jhongda Road, Jhongli City, Taoyuan County 32001, Taiwan
[b] Institute of Applied Geophysics, National Taiwan Ocean University, 2 Pei-Ning Road, Keelung 202, Taiwan

ARTICLE INFO

Article history:
Received 27 February 2013
Received in revised form 12 July 2013
Accepted 29 August 2013
Available online 7 September 2013

Keywords:
Strike-slip fault
Collision
Conjugate fault
West Philippine Sea Plate
Fracture zone
Ryukyu subduction system

ABSTRACT

On 26 April 2010, a strike-slip earthquake (Mw 6.5) occurred in the Western Philippine Sea Plate. We deployed 14 ocean-bottom seismometers to record the corresponding aftershocks to acquire information regarding these intraplate events. Our results show that the aftershocks were located along two linear features that intersect with an angle of approximately 120° and are considered a conjugate fault set. The P axis of the mainshock focal mechanism is consistent with the compressive stress direction induced by the arc–continent collision occurring in eastern Taiwan. The pre-existing oceanic fracture zones and tectonic fabrics do not appear to be reactivated based on the distinct rupture directions determined from the relocated aftershocks. However, the abrupt halt of the aftershocks at the border of the fracture zone suggests that pre-existing weak zones could act as a barrier to rupture propagation. Moreover, most large earthquakes have occurred near fracture zones, indicating that the pre-existing weakness may favor the generation of earthquakes compared to the other portion of the oceanic plate due to the relatively low rock strength of this zone.

1. Introduction

The majority of large earthquakes that occur in oceans occur at subduction zones, where one tectonic plate is thrusting beneath another. However, the 11 April 2012, Mw 8.6 and Mw 8.2 earthquakes off the west coast of northern Sumatra, Indonesia, occurred as a result of strike-slip faulting within the Indo-Australia plate. Is such a great strike-slip event within the oceanic lithosphere a special case, or could it occur elsewhere in the world? Over the last few decades, several strike-slip-type earthquakes have been observed within the West Philippine Sea Plate (WPSP) (Fig. 1). Nearly all of these earthquakes possessed a similar focal mechanism pattern with one fault plane sub-parallel to approximately N35°W–N45°W (Fig. 1b). Based on bathymetric and magnetic anomaly data, previous studies have identified several distinct tectonic structures in the WPSP, such as the Gagua Ridge, which is an ancient spreading center, and oceanic fracture zones (Deschamps et al., 2002; Hilde and Lee, 1984). However, less information regarding the present activity of these structures has been acquired. On 26 April 2010, an Mw 6.5 strike-slip-type earthquake occurred on the eastern side of Gagua Ridge (Fig. 1b), where the detectable seismic activity is generally low. To understand the earthquake mechanism, we conducted a passive ocean-bottom seismometer (OBS) experiment approximately 1 week after the occurrence of the earthquake.

2. Geological background

The Philippine Sea Plate (PHS) is moving northwestward (Yu et al., 1997) (~N306°–312°) relative to the Eurasian Plate (EU), with an 8–9 cm/yr PHS/EU plate convergence vector near Taiwan (Fig. 1). The northwestern corner of the PHS is colliding westward with the EU margin and is creating the Taiwan orogen; however, the PHS is also subducting northward beneath the Ryukyu Arc (Fig. 1a). Thus, most earthquakes in and around Taiwan are related to the convergence of these two plates (Kao and Jian, 2001; Kao et al., 1998, 2000; Kubo and Fukuyama, 2003). The Gagua Ridge, located off the eastern shore of Taiwan, is a major narrow linear high that enters the Ryukyu Arc and isolates the Huatung Basin to the west from the main West Philippine Basin (WPB) (Fig. 1b) (Deschamps and Lallemand, 2002; Dominguez et al., 1998; Hsu et al., 1996). Sibuet et al. (2002) proposed that the Gagua Ridge is a zone of weakness and could have been a plate boundary between the Philippine Sea and Huatung plates. Lin et al. (2004a, 2004b) showed that the Gagua Ridge was a former plate boundary and was sheared beneath the Ryukyu subduction zone. East of the Gagua Ridge, several major NE–SW-oriented fracture zones have been defined using bathymetric data (Hsu et al., 2013). The Luzon–Okinawa Fracture Zone (LOFZ) is the largest of these structures based on the apparent geomorphology (Fig. 1b). West of the LOFZ, the spreading fabric is illustrated by the N120°E-trending abyssal hills, which lie perpendicular to the fracture zones (Deschamps and Lallemand, 2002; Deschamps et al., 2002).

* Corresponding author. Tel.: +886 34227151x65613.
E-mail addresses: jylin.gep@gmail.com, jylin@ncu.edu.tw (J.-Y. Lin).

0040-1951/$ – see front matter © 2013 Elsevier B.V. All rights reserved.
http://dx.doi.org/10.1016/j.tecto.2013.08.038

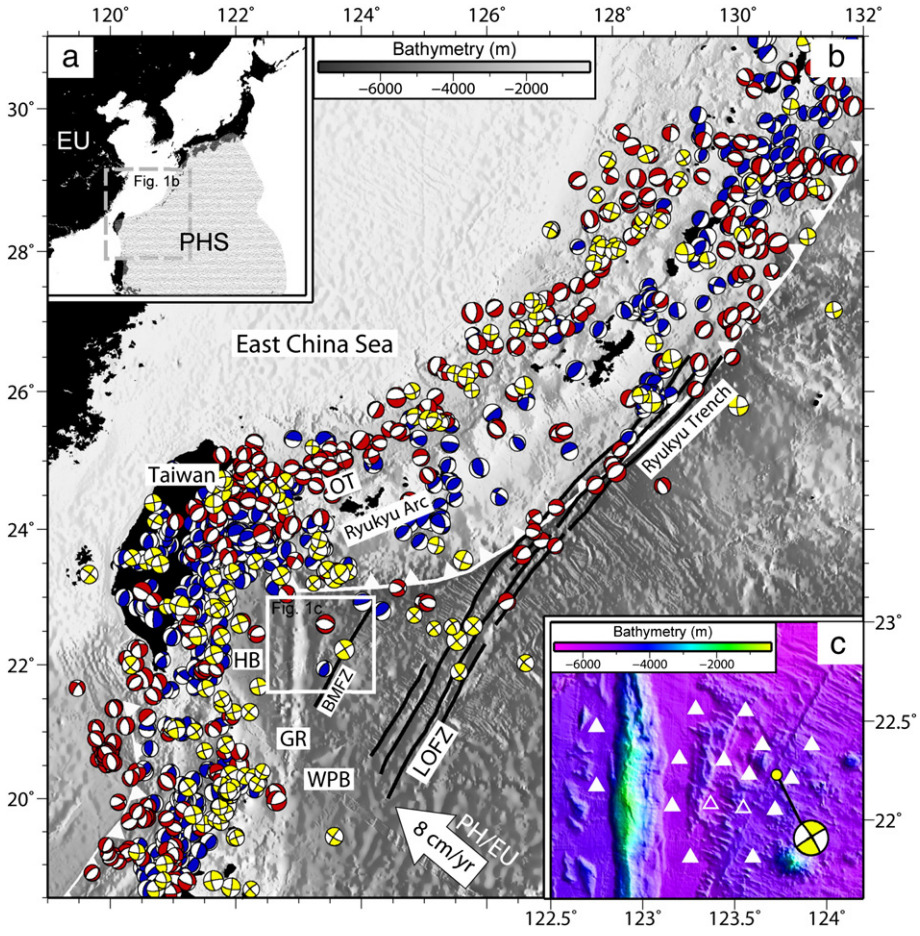

Fig. 1. (a) General map of the tectonic environment in the Western Philippine Basin. The dashed gray rectangle shows the position of (b). (b) Focal mechanisms from the Global CMT catalog (http://www.globalcmt.org/) for the period between January of 1976 and September of 2012 are plotted on the bathymetric map of the Ryukyu-Taiwan subduction–collision zone. The red, blue and yellow "beach ball" symbols show extensional, compressive and strike-slip focal mechanisms, respectively. Black lines indicate the oceanic fracture zones determined from detailed bathymetric data (Hsu et al., 2013). The detailed bathymetry of the area located in the white rectangle in (b) and the target earthquake (c) are shown. White triangles indicate the positions of the deployed OBSs. The two open triangles are the OBSs that were not successfully recovered. The white arrow shows the relative plate motion (Yu et al., 1997). The yellow focal mechanism represents the Mw 6.5 26 April 2010 mainshock with a focal depth of 24 km. EU, Eurasia; GR, Gagua Ridge; HB, Huatung Basin; LU, Luzon; LOFZ, Luzon–Okinawa Fracture Zone; BMFZ, Batan-Miyako fracture zone; OT, Okinawa Trough; PHS, Philippine Sea Plate; WPB, West Philippine Basin.

3. Data processing

We deployed 16 OBSs from May 2 to 25, 2010, within a 250 × 200 km^2 area covering parts of the West Philippine Sea Basin, Gagua Ridge and the Huatung Basin (Fig. 1c). Unfortunately, 2 OBSs were not successfully recovered (open triangles in Fig. 1c) and only 14 OBSs were used for the data processing. The spacing between OBSs varied from 18 to 60 km. Earthquake events were selected manually from continuous seismic records, and weights were assigned to P- and *S*-wave arrivals based on the quality of the signal. Events possessing more than six arrivals were initially identified using an IASP91 1-D velocity model (Kennett and Engdahl, 1991). In total, 1476 earthquakes were identified and located during an approximately 22-day record (Fig. 2a and b). However, the use of only six wave arrivals and a global 1-D velocity model may introduce manual selection and velocity errors into our localization. To improve the accuracy of the hypocenter locations, we applied the double-difference (hypoDD) method (Waldhauser and Ellsworth, 2000) to the 527 earthquakes possessing at least 10 arrivals (Fig. 2c). For this process, an appropriate 1-D velocity model of the area was derived using the seismic wave arrivals and the VELEST program (Kissling et al., 1994). The initial velocity model input for the VELEST program was extracted from the results of a wide-angle seismic reflection survey conducted in the eastern part of the Gagua Ridge (Chen, 2009). To avoid the influence of arrivals from outside of our target area, only those events that occurred around the epicenter area (~123.6–124°E; 22.1–22.5°N) were used for the inversion. During the inversion, the RMS residual decreased with each iteration and became stable after the fourth iteration (Fig. 3a). The inverted velocity model was then used as the input for the hypoDD relocation. To ensure the stability of this model, we repeated the inversion by altering the initial velocity value by as much as ±13%. The result shows that even when different initial models are used, a similar velocity value can be obtained (Fig. 3b). Finally, 326 events were relocated using the hypoDD software and the inverted 1-D velocity model (Fig. 2d). The magnitude ranged between 0.6 and 4.3, and the depth ranged from 5.4 to 34.4 km. The spatial errors of the relocation reported by hypoDD program are 13 to 558 m for the east–west, 15 to 247 m for the north–south direction and 16 to 605 m for the depth.

4. Results

4.1. Epicenter distribution

Our results show that the majority of identified earthquakes occurred in the vicinity of the April 26 mainshock area, and only a small number of events were located in the eastern Taiwan and Ryukyu subduction zones

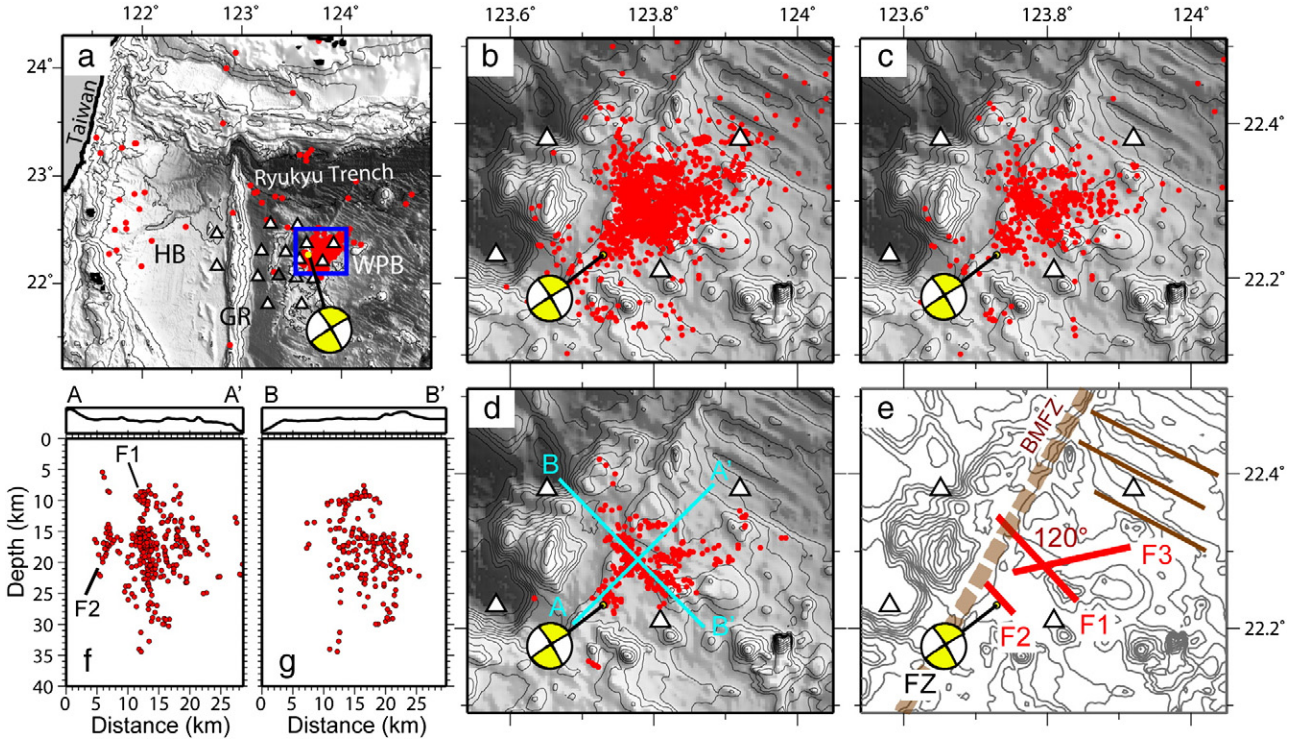

Fig. 2. Aftershock distribution. (a) Epicenters of 1476 earthquakes with at least six wave arrivals recorded by the OBS network and relocated by the 1-D IASP91 global velocity model (Kennett and Engdahl, 1991). (b) Epicenters of 1409 earthquakes located in the blue rectangle area in (a). (c) Position of 527 earthquakes possessing at least 10 arrivals and relocated by the IASP91 velocity model. (d) Positions of 326 earthquakes relocated using the hypoDD program (Waldhauser and Ellsworth, 2000) and the 1-D velocity model inverted using the VELEST program (Kissling et al., 1994). AA′ and BB′ are the positions of the two cross sections shown in (f) and (g), respectively. (e) Possible fault geometry determined by the distribution of aftershock clusters. F1, F2 and F3 are the three main clusters. The brown broad dashed lines show the ancient fracture zone and spreading fabrics determined from detailed bathymetry data (Hsu et al., 2013). The focal mechanism shown in yellow represents the Mw 6.5 26 April 2010 mainshock. (f) Earthquakes located in the 10-km-wide bandwidths on each side of the AA′ profile are plotted. (g) Earthquakes located in the 3-km-wide bandwidths on each side of the BB′ profile are plotted. The figure located in the upper portion of (f) and (g) shows the bathymetry of the two cross sections.

(Fig. 2a). This result could be due to the relatively great distance between our network and the two tectonically active areas. No event was reported by the global CMT catalog (http://www.globalcmt.org/) and only 8 earthquakes have been recorded by the International Seismological Center catalog (ISC, http://colossus.iris.washington.edu/) in our study area during the recording period, indicating the relatively small magnitude of earthquakes collected by our network. After the relocation, the distribution of the aftershocks appeared to be more concentrated (Fig. 2d). The most obvious earthquake cluster is a N45°W trending, approximately 19-km long feature (F1 in Fig. 2e) crossing the latitude range between

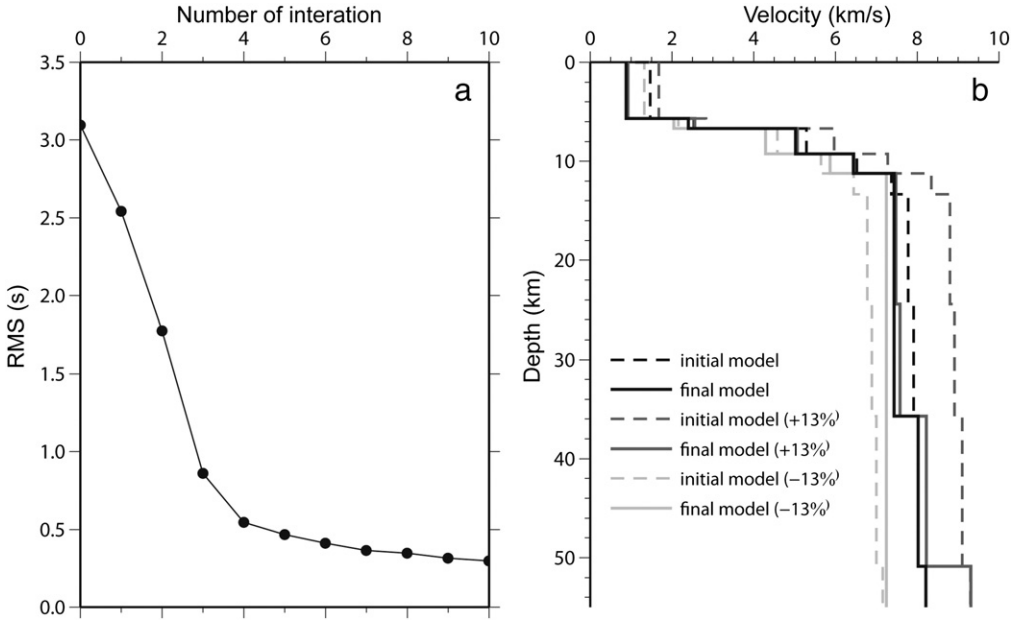

Fig. 3. (a) RMS distribution as a function of the number of iterations during the 1-D velocity inversion using the VELEST program. (b) Initial input velocity model (dashed lines) and their corresponding inverted model (solid lines). The inversion was performed by varying the initial velocity value by ±13%.

approximately 22.25°N and 22.35°N. Southwest of the cluster, in the vicinity of 22.24°N, is another cluster characterized by a relatively small length of approximately 6 km (F2) that extends along a direction subparallel to that of F1. The third cluster (F3), occurring along a 17-km-long path, intersects F1 at an angle of approximately 120°. Regardless of the earthquake cluster, the western prolongation of these earthquakes appears to be restricted by a NNE–SSW-trending fracture zone (Fig. 2d).

4.2. Cross section

Two vertical cross sections, one oriented in a NE–SW direction and the other in a NW–SE direction, are shown in Fig. 2f and g (AA′ and BB′). The vertical distribution of earthquakes along Profile AA′ shows that the F1 and F2 earthquake clusters belong to two 3-km-wide strips (Fig. 2f). F1 is characterized by a larger depth range of 8–35 km compared with the range of 15–25 km for the F2 feature. All other earthquakes occurred at depths of 10 to 25 km. The depth distribution pattern shows that F1 is likely the most important seismic structure, having the largest rupture extent, and can pass through the oceanic crust to the lithosphere. The NW–SE Profile BB′ shows that the earthquakes of F1 become deeper toward the southeast (Fig. 2g). The lower limit is from 17 km for the most northwestern area, near the oceanic fracture zone, to 30 km in the southeastern portion. In addition, both profiles show relatively low seismicity in the depth range of 11–14 km.

5. Discussion

5.1. Fault plane determination based on the aftershock distribution

Based on the concentration and size of the aftershock distribution, we observed that the majority of the post-seismic activity occurred along F1 and F2, two N45°W trending linear features (Fig. 2e). The presence of a small bathymetric scrape trending along F1 is also indicative of active deformation along this structure (Figs. 2d and 4c). Therefore, we propose that the main rupture should propagate in a NW–SE direction, which is consistent with the NW–SE fault plane solution of the Global Centroid Moment Tensor (CMT) focal mechanism (http://www.globalcmt.org/) for the mainshock. In this case, a sinistral rupture along an approximately vertical fault plane is determined for the 26 April 2010 Mw 6.5 earthquake. Moreover, the strike-slip events, observed in the vicinity of the LOFZ area approximately 200 km east of our study area, are characterized by similar focal mechanisms (Fig. 4b) (Lin et al., 2013). The background seismicity and swath-bathymetric features of this area also indicate a NW–SE fault plane (Matsumoto et al., 2001). Consequently, the predominance of NW–SE tectonic structures in the Western Philippine Basin is revealed. Meanwhile, some NWW–SEE bathymetric lineaments, representing the former tectonic fabrics, are observed on each side of the fracture zone (the brown lines in Fig. 2e). We noticed that the orientation of these tectonic fabrics is not in parallel with F1 and F2 (Fig. 2e), suggesting that the occurrence of aftershocks could not be correlated to the reactivation of the ancient pre-existing features.

It is worth noting that F1 appears to be the most widely distributed seismically active feature, along with the reported epicenter of the mainshock located in F2, and is a relatively small cluster (Fig. 2d). This phenomenon can be discussed from two different perspectives: (1) In the marine area, possible earthquake location errors could be generated by an inaccurate velocity model and poor ray coverage. Thus, a hypocentral mislocation may have occurred, and the hypocenter of the mainshock should be located farther north in the position of F1. (2) The mainshock did occur in F2 and triggered the activity along F1. As determined by the aftershock distribution, the physical dimension of F2 is estimated to be about 5 km by 8 km, whereas the F1 is about 15 km by 20 km (Fig. 4c). Given a normal value of rigidity at the source location and a normal stress drop, the fault area of a Mw 6.5 event is expected to be

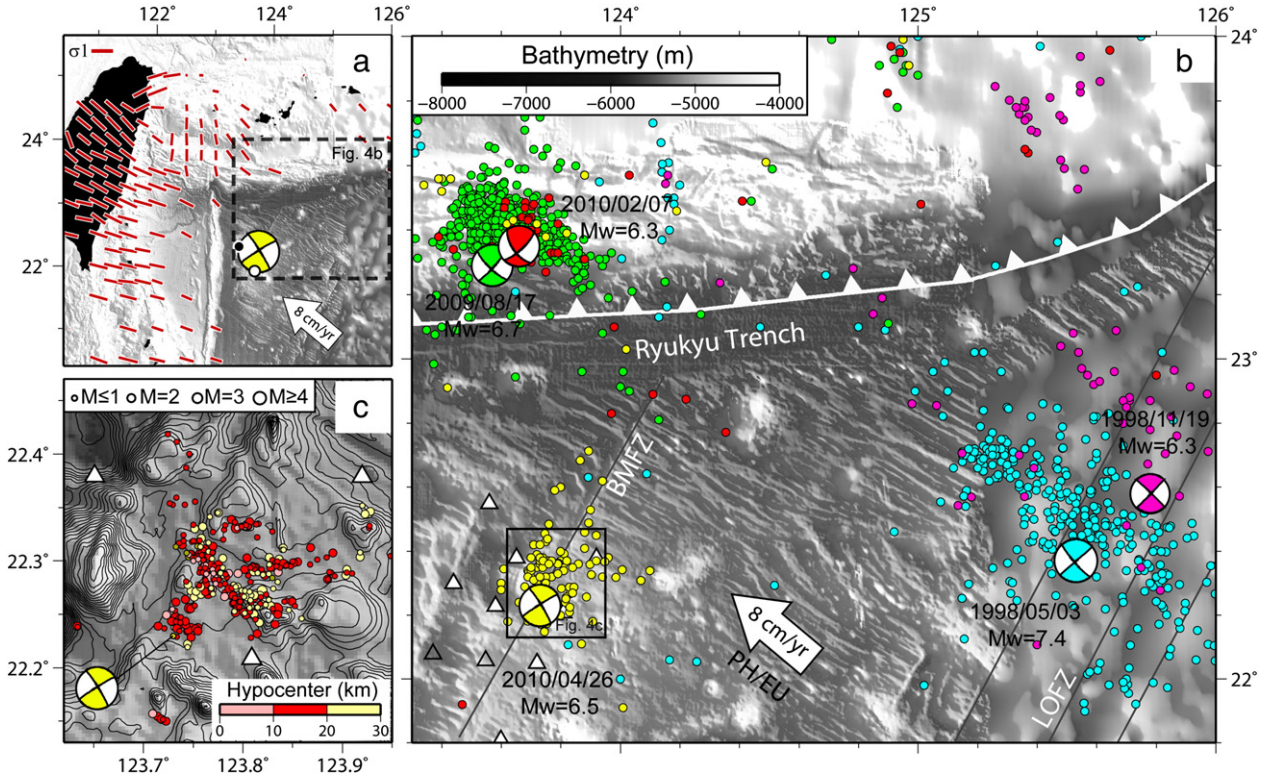

Fig. 4. (a) Principal compressive stress distribution (red lines) inverted by Wu et al. (2010) in the Ryukyu Taiwan collision zone. The length of the red lines is proportional to the horizontal component. The focal mechanism shown in yellow corresponds to the Mw 6.5 26 April 2010 mainshock. The black and white dots show the direction of the P and T axes of the mainshock. (b) Focal mechanisms of the earthquakes located in the Philippine Sea Plate with magnitudes larger than six are plotted using different colors. Aftershocks occurring within one month after the occurrence of the mainshock are plotted using the same color. The white arrow shows the relative plate motion (Yu et al., 1997). (c) Relocated aftershock distribution plotted as a function of its magnitude. Triangles indicate the OBS positions.

on the order of 100–200 km^2, which is closer to the dimension of F1. Moreover, the fault area inferred from aftershock distribution is somewhat larger than that inferred from the theoretical fault model for most case. Therefore, it seems that F1 is a better candidate for the preferred rupture plane. Furthermore, it is widely accepted that most of the accumulated stress on the rupture area has been released during the mainshock. Thus, it is expected that aftershocks inside the main rupture zone are relatively smaller than those on the peripheral of the rupture zone. Consequently, we identify the F1 nodal plane as the preferred rupture plane rather than F2.

5.2. Conjugate fault and tectonic stress regime

As described previously, the relocated epicenters are mainly distributed along two linear features that intersect at angles of approximately 60° and 120° (Fig. 2e). This cross-cutting set of fault planes can be understood as a conjugate fault set: the dominant set, known as F1 and F2, forms in the NW direction and is then linked by a second set, the F3 feature, located along a NE alignment. This type of conjugate fault has been reported in several oceanic plates. For examples, the large June 18, 2000, Mw 7.9 (13.87°S, 97.3°E) earthquake in the Wharton basin and the 11 April 2012, Mw 8.6 and Mw 8.2 earthquakes off the west coast of northern Sumatra appear to have involved predominantly left-lateral strike-slip faulting along the expected NNE–SSW orientation, although a second fault orientation was also activated (Pollitz et al., 2012; Robinson et al., 2001; Satriano et al., 2012; Yue et al., 2012). Moreover, in November of 1987, an Mw 7.2 earthquake on a fault trending approximately E–W in the Gulf of Alaska was followed less than 2 weeks later by an Mw 7.8 earthquake on the conjugate N–S fault (Pegler and Das, 1996). Generally, if strike-slip faults are formed by the Coulomb fracture mechanism, which predicts the formation of X-shaped shear fractures 30° from the σ1 direction, the intersection angles between conjugate strike-slip faults should be approximately 60° and 120° (Donath, 1961; Sibson et al., 1988; Yin and Ranalli, 1992). This mechanism is in complete agreement with the result obtained from our study.

To determine the origin of the present-day stress regime of our study area, we compared the P axis orientation obtained from the focal mechanism of the 2010 mainshock (black dot in Fig. 4a) with the principle compressive stress directions inverted by Wu et al. (2010) for the westernmost portion of the WPSP area (red bars in Fig. 4a). As shown in Fig. 4a, the σ1 direction is maintained within 5° from the relative plate motion for the majority of central Taiwan. However, due to the tectonic compression induced by the collision between the Luzon Arc and the Eurasia Plate in the southeastern region of Taiwan, the σ1 direction deviated counterclockwise from an NW–SE to an almost E–W direction (Wu et al., 2010), which is consistent with the P axis orientation of the mainshock and other strike-slip events occurring in the WPSP. Based on the local seismicity and fault plane solutions, this approximately E–W-trending compressional direction was also identified by Kao et al. (1998) for eastern Taiwan and offshore areas and was considered an effect of collision. The evidence of this E–W regional stress regime can also be observed in the faulting geometries shown by the three main earthquake clusters determined in our study. The three clusters show steeply dipping strike-slip orientations having either a left-lateral slip on NW–SE faults (Faults F1 and F2) or a right-lateral slip on ENE–WSW faults (Fault F3), both are consistent with the pervasive E–W compressional stress orientation throughout the region. Consequently, the arc–continent collision process between the Luzon Arc and the Eurasia Plate may be the origin of the stress regime for the intraplate events located within the WPSP. Hence, a similar focal mechanism possessed by the strike-slip events, observed between longitudes of approximately 123° and 126°, may suggest that the resisting force of the collision is transmitted over a distance of approximately 500 km from eastern Taiwan to the LOFZ area (Fig. 4b). This type of stress transfer was previously reported for the Wharton Basin and offshore northern Sumatra, where the compressional axes of earthquakes are consistently oriented in a NW–SE direction. This orientation indicates that the intraplate stresses in the region are primarily inherited from the India-Asia collision over a distance of approximately several thousand kilometers (Deplus et al., 1998; Robinson et al., 2001).

To extend our discussion, we put forward several questions.

First, in other oceanic plates around the world, such as in the Gulf of Alaska and the Wharton Basin, most intraplate earthquakes have occurred along a reactivated relic transforms and relic ridges. However, based on our results, no obvious seismic activity occurred along the former tectonic structures in the WPSP area (Fig. 2a). All of the ancient tectonic structures in the WPSP appear to be seismically inactive in the present day. For example, a portion of the Gagua Ridge is located in our network and is surrounded by the six western-most OBS stations; however, only a faint earthquake was recorded along this structure during our recorded period. Moreover, the orientation of the earthquake clusters determined from the OBS data does not appear to extend along the oceanic fracture zones or fabrics but has an intersecting angle (Fig. 4b). Thus, the first question raised is why the oceanic fracture zones in the WPSP, which represent the tectonically weak area, have not been reactivated by the earthquakes that have occurred within the oceanic plate. In the WPSP as well as in the other tectonic areas, we note that the P axis of the focal mechanisms is consistent with the direction of collision regardless of the orientation of pre-existing weak zones. Therefore, we propose that the regional principle stress direction is the main factor controlling the active fault plane orientation in the present day, and the influence of the pre-existing fracture zones should be minor. However, the presence of the pre-existing weakness continues to have certain effects on the distribution of large strike-slip events. For example, as shown by our results, almost all of the recorded aftershocks stop suddenly on the eastern side of a fracture zone, indicating that the pre-existing features could act as a barrier to rupture propagation. In addition, we note that the majority of relatively large earthquakes occurred within the vicinity of the oceanic fracture zones (Fig. 4b), suggesting that the pre-existing weak zone may favor the generation of earthquakes due to its relatively low rock strength compared with the compact, un-ruptured oceanic plate.

In addition, based on the previous discussion, we found that the tectonic context within the WPSP area is similar to that in the Wharton Basin: shortening by thrust earthquakes occurs on the western side, and the oceanic lithosphere subducts along the trench system on the other side. This tectonic environment could be the cause of the similar characteristics of the intraplate earthquakes located within the two oceanic areas. Consequently, analogous interactions between the underthrusting events at the subduction interface and intraplate deformation offshore may be expected for these two areas. Delescluse et al. (2012) demonstrated that the 11 April 2012 twin strike-slip earthquakes were part of a continuing enhancement of the intraplate deformation between India and Australia that followed the Ache 2004 and Nias 2005 megathrust earthquakes. Will a similar tectonic process occur along the Ryukyu subduction system? What do these earthquakes reveal about earthquake physics, and how might they change earthquake hazard assessment? All of these questions are crucial and require further investigation.

6. Conclusions

On 26 April 2010, a strike-slip-type earthquake (Mw 6.5) occurred on the eastern portion of the Gagua Ridge. We deployed 14 OBSs to record the aftershocks to acquire information regarding these strike-slip earthquakes in the oceanic plate. A total of 326 aftershocks were relocated based on the hypoDD analysis, and an appropriate 1-D velocity model of the area was derived using the VELEST program. Our results show that the majority of identified earthquakes occurred in the vicinity of the mainshock area. Three clusters of earthquakes were identified: two of them trend along the N45°W direction, and the other intersects the first two clusters at an angle of approximately 120°. The origin of the stress regime is evidenced by the consistency of the P axis of the focal

mechanism for the mainshock and the principle compressive stress resulting from the collision occurring in southeastern Taiwan. Thus, the diffuse intraplate seismicity in this WPSP region should result from the collision between the Luzon Arc and the Eurasia continental margin. In addition, the influence of this collision process appears to have reached the LOFZ area, approximately 500 km from the eastern coast of Taiwan, over a very long distance. Because the strike of the earthquake clusters is distinct from that of the ancient tectonic features, the seismicity does not appear to be linked to their reactivation. However, the abrupt halt of the aftershock distribution at the border of the fracture zone suggests that the pre-existing features could act as a barrier to the rupture propagation. In addition, most large earthquakes occurred within the vicinity of the oceanic fracture zones, suggesting that the pre-existing weak zone may favor the generation of earthquakes due to the relatively low rock strength compared with the compact, un-ruptured oceanic plate.

Acknowledgement

We thank Dr. Honn Kao and an anonymous reviewer for their careful reviews which help a lot to improve this manuscript. Pertinent discussions with Dr. Wen-Nan Wu, Chung-Liang Lo and Wen-Bin Doo are acknowledged. We are grateful to Dr. Wen-Tzong Liang for providing us assistance with data processing. Figures were prepared with the Generic Mapping Tool (GMT) software (Wessel and Smith, 1998). This research was supported by the Taiwan Earthquake Research Center (TEC) funded through the National Science Council (NSC) with grant numbers NSC-102-3113-P-008-006 and NSC-102-2116-M-008-024. The TEC contribution number for this article is 00096.

References

Chen, T.R., 2009. OBS Imaging of Crustal Velocity Structures Along Eastern and Western Troughs of the Gagua Ridge. Master thesis Institute of Applied Geosciences, National Taiwan Ocean University, 58 pp (in Chinese).

Delescluse, M., Chamot-Rooke, N., Cattin, R., Fleitout, L., Trubienko, O., Vigny, C., 2012. April 2012 intra-oceanic seismicity off Sumatra boosted by the Banda-Aceh megathrust. Nature 490, 240–244.

Deplus, C., Diament, M., Hébert, H., Bertrand, G., Dominguez, S., Dubois, J., Malod, J., Patriat, P., Pontoise, B., Sibilla, J.J., 1998. Direct evidence of active deformation in the eastern Indian oceanic plate. Geology 26, 131–134.

Deschamps, A., Lallemand, S., 2002. The West Philippine Basin: an Eocene to early Oligocene back arc basin opened between two opposed subduction zones. J. Geophys. Res. 107. http://dx.doi.org/10.1029/2001JB001706.

Deschamps, A., Okino, K., Fujioka, K., 2002. Late amagmatic extension along the central and eastern segments of the West Philippine Basin fossil spreading axis. Earth Planet. Sci. Lett. 203, 277–293.

Dominguez, S., Lallemand, S., Malavieille, J., Schnurle, P., 1998. Oblique subduction of the Gagua Ridge beneath the Ryukyu accretionary wedge system: insights from marine observations and sandbox experiments. Mar. Geophys. Res. 20, 383–402.

Donath, F.A., 1961. Experimental study of shear failure in anisotropic rocks. Geol. Soc. Am. Bull. 72, 985–989.

Hilde, T.W.C., Lee, C.-S., 1984. Origin and evolution of the West Philippine Basin: a new interpretation. Tectonophysics 102, 85–104.

Hsu, S.-K., Sibuet, J.-C., Monti, S., Shyu, C.-T., Liu, C.-S., 1996. Transition between the Okinawa trough backarc extension and the Taiwan collision: new insights on the southernmost Ryukyu subduction zone. Mar. Geophys. Res. 18, 163–187.

Hsu, S.-K., Yeh, Y.-C., Sibuet, J.-C., Doo, W.-B., Tsai, C.-H., 2013. A mega-splay fault system and tsunami hazard in the southern Ryukyu subduction zone. Earth Planet. Sci. Lett. 362, 99–107.

Kao, H., Jian, P.-R., 2001. Seismogenic patterns in the Taiwan region: insights from source parameter inversion of BATS data. Tectonophysics 333, 179–198.

Kao, H., Shen, S.S.-J., Ma, K.-F., 1998. Transition from oblique subduction to collision: earthquakes in the southernmost Ryukyu arc–Taiwan region. J. Geophys. Res. 103, 7211–7229.

Kao, H., Huang, G.-C., Liu, C.-S., 2000. Transition from oblique subduction to collision in the northern Luzon arc–Taiwan region: constraints from bathymetry and seismic observations. J. Geophys. Res. 105, 3059–3079.

Kennett, B.L.N., Engdahl, E.R., 1991. Traveltimes for global earthquake location and phase identification. Geophys. J. Int. 105, 429–465.

Kissling, E., Ellsworth, W., Eberhart-Phillips, D., Kradolfer, U., 1994. Initial reference models in local earthquake tomography. J. Geophys. Res. 99, 19635–19646.

Kubo, A., Fukuyama, E., 2003. Stress field along the Ryukyu Arc and the Okinawa Trough inferred from moment tensors of shallow earthquakes. Earth Planet. Sci. Lett. 210, 305–316.

Lin, J.-Y., Hsu, S.-K., Sibuet, J.-C., 2004a. Melting features along the Ryukyu slab tear, beneath the southwestern Okinawa Trough. Geophys. Res. Lett. 31, L19607. http://dx.doi.org/10.1029/2004GL020862.

Lin, J.-Y., Hsu, S.-K., Sibuet, J.-C., 2004b. Melting features along the western Ryukyu slab edge (northeast Taiwan): tomographic evidence. J. Geophys. Res. 109. http://dx.doi.org/10.1029/2004JB003260.

Lin, J.-Y., Hsu, S.-K., Sibuet, J.-C., Lee, C.-S., Liang, C.-W., 2013. Plate tearing in the northwestern corner of the subducting Philippine Sea Plate. J. Asian Earth Sci. 70–71, 1–7.

Matsumoto, T., Kimura, M., Nakamura, M., Ono, T., 2001. Large-scale slope failure and active erosion occurring in the southwest Ryukyu fore-arc area. Nat. Hazards Earth Syst. Sci. 1, 203–211.

Pegler, G., Das, S., 1996. Analysis of the relationship between seismic moment and fault length for large crustal strike-slip earthquakes between 1977-92. Geophys. Res. Lett. 23, 905–908.

Pollitz, F.F., Stein, R.S., Sevilgen, V., Bürgmann, R., 2012. The 11 April 2012 east Indian Ocean earthquake triggered large aftershocks worldwide. Nature 490, 250–253.

Robinson, D., Henry, C., Das, S., Woodhouse, J., 2001. Simultaneous rupture along two conjugate planes of the Wharton Basin earthquake. Science 292, 1145–1148.

Satriano, C., Kiraly, E., Bernard, P., Vilotte, J.P., 2012. The 2012 Mw 8.6 Sumatra earthquake: evidence of westward sequential seismic ruptures associated to the reactivation of a NS ocean fabric. Geophys. Res. Lett. 39, L15302.

Sibson, R.H., Robert, F., Poulsen, K.H., 1988. High-angle reverse faults, fluid-pressure cycling, and mesothermal gold-quartz deposits. Geology 16, 551–555.

Sibuet, J.-C., Hsu, S.-K., Le Pichon, X., Le Formal, J.-P., Reed, D., Moore, G., Liu, C.-S., 2002. East Asia plate tectonics since 15 Ma: constraints from the Taiwan region. Tectonophysics 344, 103–134.

Waldhauser, F., Ellsworth, W.L., 2000. A double-difference earthquake location algorithm: method and application to the northern Hayward fault. Bull. Seismol. Soc. Am. 90, 1353–1368.

Wessel, P., Smith, W.H., 1998. New, improved version of Generic Mapping Tools released, Eos Trans. AGU 79, 579-579.

Wu, W.-N., Kao, H., Hsu, S.-K., Lo, C.-L., Chen, H.-W., 2010. Spatial variation of the crustal stress field along the Ryukyu–Taiwan–Luzon convergent boundary. J. Geophys. Res. 115, B11401.

Yin, Z.M., Ranalli, G., 1992. Critical stress difference, fault orientation and slip direction in anisotropic rocks under non-Andersonian stress systems. J. Struct. Geol. 14, 237–244.

Yu, S.-B., Chen, H.-Y., Kuo, L.-C., 1997. Velocity field of GPS stations in the Taiwan area. Tectonophysics 274, 41–59.

Yue, H., Lay, T., Koper, K.D., 2012. En echelon and orthogonal fault ruptures of the 11 April 2012 great intraplate earthquakes. Nature 490, 245–249.